Appl Biochem Biotechnol (2015) 176:344–358
DOI 10.1007/s12010-015-1578-2

Highly Selective Electrochemical Determination of Taxol Based on ds-DNA-Modified Pencil Electrode

M. Taei[1] · F. Hassanpour[1] · H. Salavati[1] · Z. Sadeghi[1] · H. Alvandi[1]

Received: 2 December 2014 / Accepted: 12 March 2015 /
Published online: 1 April 2015

Abstract In this research, TiO_2/ZrO_2 nanocomposite has been prepared using sol-gel method. The TiO_2/ZrO_2 composite was characterized by X-ray diffraction (XRD), Fourier transform infrared spectroscopy (FT-IR), and transmission electron microscopy (TEM). A sensitive electrochemical biosensor is also presented for the determination of Taxol based on ds-DNA decorated multiwall carbon nanotubes-TiO_2/ZrO_2–chitosan-modified pencil electrode (ds-DNA-MWNTs-TiO_2/ZrO_2–CHIT-PGE). The UV spectroscopic data and differential pulse voltammetry revealed that there is a strong interaction between ds-DNA and Taxol. The groove binding of Taxol to ds-DNA helix has been characterized by a red shift (less than 8 nm) in wavelength and the decrease in the differential pulse voltammetry oxidation signal intensity of the Taxol at pencil graphite electrode (PGE) after its interaction with ds-DNA. Finally, a pretreated PGE modified with ds-DNA-MWNTs-TiO_2/ZrO_2–CHIT was tested in order to determine Taxol content in the solution. The dynamic range was from 0.7 to 1874.0 nmol L^{-1} with a detection limit of 0.01 nmol L^{-1}. This sensing platform was successfully applied for the determination of Taxol in pharmaceutical and biological samples.

Keywords Biosensor · TiO_2/ZrO_2 nanocomposite · Chitosan-modified multiwall carbon nanotubes · Voltammetry

Introduction

Carbon nanotubes with high surface area, excellent electron transport capacity, high chemical stability, and outstanding catalytic ability have also been widely used in biosensors [1, 2]. In carbon nanotubes, properties can be improved or tuned toward

✉ M. Taei
m.taei@ch.iut.ac.ir; m_taei57@yahoo.com

[1] Chemistry Department, Payame Noor University, 19395-4697 Tehran, Iran

specific purposes by chemical modification [3] when mixed with another material, especially in transition metal nanoparticles, which are known for their catalytic properties toward detection and determination of both environmental and biological analytes [4–9]. The distribution of these metal nanoparticles is increased due to their larger surface area when they are supported on carbon nanotubes. In addition, chitosan (CHIT), a naturally derived biopolymer, serves as a matrix for the assembly of biomolecules, nanoparticles, and other substances. Many studies combine chitosan with carbon nanotubes and metal oxides for the electrochemical biosensing platforms [10–12].

After the discovery of electroactivity of nucleic acids, there has been a growing interest in the electrochemical investigation of interaction between anticancer drugs and DNA. In these techniques, DNA-electrochemical biosensors are one of the most important groups, which comprise a nucleic acid recognition layer immobilized over an electrochemical transducer. Different immobilization procedures such as formation of monolayer or multilayer DNA film, electrostatic adsorption, and evaporation and incubation procedure in the solution are used for electrode surface modification. These investigations are based on the differences in the electrochemical DNA and drug behaviors such as decrease and increase in the peak currents and shifts of potentials. Therefore, biosensors have been successfully used to identify the interaction of anticancer drug with DNA [13].

Paclitaxel (Taxol) is a mitotic inhibitor used in cancer chemotherapy; this and docetaxel represent the taxane family of drugs [14]. Paclitaxel's mechanism of action involves its stabilization of cellular microtubules; as a result, it interferes with the normal breakdown of microtubules during cell division. Paclitaxel is used to treat patients with lung, ovarian, breast, and head and neck cancers, and advanced forms of Kaposi's sarcoma. It is also used for the prevention of restenosis. Electrochemical determination of paclitaxel is a promising candidate because its quinone and hydroquinone groups are chemically active. Furthermore, electrochemical methods have advantages such as simplicity, speed, and sensitivity [15–21].

Recently, several papers have introduced new modified electrodes for the determination of Taxol including DNA immobilized onto the azide-terminated monolayers-modified gold electrode [15], cysteamine/DNA/single-walled carbon nanotubes film-modified gold electrode [17], and hemoglobin on didodecyldimethylammonium bromide/single-walled carbon nanotubes film-modified gold electrode [19]. However, these methods suffered from serious problems such as expensive chemical materials for electrode modification, toxicity, and being time consuming.

Review of literature revealed that the electrochemical behavior of Taxol at pencil graphite electrode exhibits a well-defined anodic peak at about +1.21 V at pH 7.0 by cyclic voltammetry. The intensity of the obtained peak is better compared to the peak at carbon paste electrode and glassy carbon electrode because of higher electro-active surface [18, 21]. Therefore, the pencil graphite electrode has been successfully applied to be the working electrode for this paper. We also successfully prepared the TiO_2/ZrO_2 nanocomposite by using the sol-gel method [22]. Then, DNA biosensor was constructed for the determination of Taxol. For this purpose, a mixture of multiwall carbon nanotubes (MWNTs), TiO_2/ZrO_2 and chitosan was immobilized on the surface of a PGE to improve the immobilization of ds-DNA on the surface. The experimental result showed that MWNTs-TiO_2/ZrO_2–CHIT nanocomposite graphite electrode could obviously promote the electrochemical response of Taxol compared to MWNTs-TiO_2–CHIT-PGE, MWNTs-

ZrO_2–CHIT-PGE, and MWNTs–CHIT-PGE. Furthermore, the interaction of Taxol with DNA has been studied by differential pulse voltammetry as well as UV-Vis spectroscopy.

Experimental

Chemicals and Apparatus

All voltammetric measurements were carried out using an electrochemical system comprising the Metrohm instrument (Herisau, Switzerland), Model 797 *VA*, and a conventional three-electrode cell assembly (Ag/AgCl electrode as reference electrode, a platinum wire as counter electrode and ds-DNA decorated multiwall carbon nanotubes-TiO_2/ZrO_2–chitosan-modified pencil electrode (ds-DNA-MWNTs-TiO_2/ZrO_2–CHIT-PGE) as working electrode.

Stock solutions of Taxol (Sigma-Aldrich company) were prepared by dissolving accurately weighed Taxol in methanol. The solution was conserved at −20 °C, covered with aluminum foil and left to attain room temperature before use. Taxol working solutions for voltammetric investigations were prepared by the dilution of the stock solution with phosphate buffer (pH 7.0) containing 0.02 mol L^{-1} NaCl. Reagent grade Tris–HCl, CH_3COOH, CH_3COONa, HNO_3, EDTA, NaCl, $K_3Fe(CN)_6$, $K_4Fe(CN)_6$, and NaOH were purchased from Aldrich Chemicals (Milwaukee, USA).

A calf thymus ds-DNA (Sigma-Aldrich company) stock solution was prepared in Tris buffer (TE, pH 7.0) and kept frozen. More diluted solutions of the ds-DNA were prepared with phosphate buffer (pH 7.0) containing 0.02 mol L^{-1} NaCl. Furthermore, this ds-DNA solution was heated in a water bath at 100 °C for 30 min and cooled in an ice bath immediately to prepare single strain DNA [23].

Synthesis Procedure for Preparing TiO_2/ZrO_2 Nanocomposite and Characterizations

ZrO_2/TiO_2 (1/1) was prepared by the sol–gel method. Zirconium(IV) isopropoxide (70 wt% solution in 2-propanol) and titanium(IV) *n*-butoxide (99 %) were used as precursors, and 2,4-pentandione (H-acac) was used as the complexing agent [22, 24]. Appropriate amounts of zirconium propoxide and titanium *n*-butoxide were dissolved in the solvent, *n*-butanol. The solution was heated to 60 °C, and the components were thoroughly mixed. Then, the solution was cooled down to room temperature and calcined at 500 °C for 5 h. After that, the structural and morphological properties of nanocomposite were characterized by XRD, TEM, and FT-IR.

Preparation of MWNTs-TiO_2/ZrO_2–CHIT Modified Graphite Electrode

To eliminate metal oxide catalysts within the nanotubes, multiwalled carbon nanotubes were refluxed in the 2.0 M HNO_3 for 15 h and then washed with twice-distilled water and dried at room temperature. Nitric acid usually causes a significant destruction of carbon nanotubes and introduces –COOH and –OH groups at the ends or at the sidewall defects in the nanotube structure, and carbon nanotubes would be hydrophilic after treatment.

A 2 % chitosan solution was prepared in 1 % acetic acid. Then, MWNTs (1.0 mg mL^{-1}) and TiO_2/ZrO_2 nanocomposite (0.5 mg mL^{-1}) were dissolved in chitosan solution under 3 h

sonication to obtain a homogeneous black suspension, which was sonicated for 15 min immediately before preparing the MWNTs-TiO_2/ZrO_2–CHIT films. PGE was dipped into this composite for 30 min. Then, the electrode was washed with deionized water and dried. After that, the graphite electrode was immersed in 0.1 M NaOH for 15 min to make the film more stable. Afterward, the electrode was rinsed with double-distilled water three times and air-dried.

Calf Thymus DNA Immobilization

The body of the pencil lead was tightly coated with Teflon band. Electrical contact with the lead was achieved by soldering a copper wire to the metal holder of the working electrode. The pencil lead was then fixed vertically and immersed into a solution in which the contact was only achieved via the cross section of the electrode. The surface of PGE was pretreated by applying +1.80 V for 300 s in a quiescent solution of 0.5 mol L^{-1} acetate buffer containing 0.02 mol L^{-1} NaCl (pH 4.8). This treatment led to further and better absorption of biomolecules, nanoparticles, and polymers on the PGE [25].

All Calf thymus DNA solutions (10.0 μg mL^{-1}) were prepared in TE buffer (pH 7.0). The modified graphite electrode was immersed in the DNA solution under stirring for 30 min at room temperature. Then, the electrode was washed with TE buffer three times. This modified PGE was designated as ds-DNA-MWNTs-TiO_2/ZrO_2–CHIT-PGE. Microscopic area of the ds-DNA-MWNTs-TiO_2/ZrO_2–CHIT-PGE was obtained by CV using 1 mM $K_3Fe(CN)_6$ as a probe at different scan rates. For a reversible process, Randles-Sevcik formula was used:

$$I_{pa} = 2.69 \times 10^5 n^{3/2} A C_0 D_R^{1/2} \nu^{1/2} \quad (1)$$

where I_{pa} refers to the anodic peak current, n refers to the electron transfer number, A refers to the surface area of the electrode, D_R refers to the diffusion coefficient, C_0 refers to the concentration of $K_3Fe(CN)_6$, and ν is the scan rate. For 1 mM $K_3Fe(CN)_6$ in the 0.1 M KCl electrolyte, n=1 and D_R=7.6×10^{-6} cms^{-1}. Then, from the slope of the I_{pa} $-\nu^{1/2}$ relation, the microscopic areas were calculated. The electrode surface was found 0.335 cm^2 for ds-DNA-MWNTs-TiO_2/ZrO_2–CHIT modified PGE.

Preparation of Real Samples

Serum samples were obtained and stored frozen until the analysis time. For the preparation of serum samples, 1.0 mL of each sample was diluted to 10.0 mL in voltammetric flask by phosphate buffer solution (pH 7.0). Then, 5 mL of this solution was transferred to the voltammetric cell and was diluted to 10 mL with phosphate buffer solution. To this solution, different amounts of Taxol were added, and the recovery percent was obtained by DPV technique and standard addition method.

The urine sample was collected from a healthy person and was centrifuged (10 min at 1200 rpm). After filtering, it was diluted ten times with doubly distilled water and was used without any additional pretreatment. A 0.5 mL of each sample was used in each experiment, and the pH was adjusted by 4.5 mL of 0.1 M PBS solution with

pH 7.0. The standard addition method was used to determine Taxol in the spiked samples.

The Taxol injection solution samples (labeled 6 mg mL^{-1}, Bristol-Myers Squibb) were diluted 100 times with buffer solution pH 7.0. Then, 70 μL of the solution plus 5 mL of the buffer (pH 7.0) was diluted with water in a 10-mL volumetric flask, and the resulting solution was placed in an electrochemical cell to determine their concentrations using the DPV method.

Results and Discussion

Characteristics of TiO_2/ZrO_2 Composite

The TEM image of the synthesized TiO_2/ZrO_2 nanocomposites is shown in Fig. 1a. Each of these pale dark particles was less than 50 nm. The TiO_2 sample consisted of irregularly shaped particles with a wide range of sizes [26]. In contrast, TiO_2/ZrO_2 nanocomposites comprised uniformly sized particles in a spherical structure smaller than that of the TiO_2 sample. In fact, the addition of ZrO_2 can effectively suppress the growth of TiO_2 crystals and stabilizing their structure [26].

The structure of TiO_2/ZrO_2 composite was investigated by the XRD experiment. Figure 1b shows the XRD patterns of the TiO_2/ZrO_2 sample prepared after calcinations at 500 °C. All the diffraction peaks are in agreement with the JCPDS No. 21-1272 and JCPDS file ((JCPDS No. 42-1164), which can be indexed as an anatase phase of TiO_2 and the tetragonal phase of ZrO_2.

FT-IR was employed to further characterize the as-made TiO_2, ZrO_2, and TiO_2/ZrO_2 composites. The TiO_2 nanoparticles show a strong and wide absorption band at around 600 cm^{-1} possibly resulting from the stretching vibration of O–Ti–O. The change of this strong absorption band and the appearance of new bonds at around 420 and 750 cm^{-1}, possibly caused by the stretching vibration of Zr–O bond, provide additional evidence for the successful synthesis of TiO_2/ZrO_2 (Fig. 1).

Optimization of Parameters in the Determination of Taxol

For the optimal conditions of Taxol detection, the present electrochemical sensor was optimized in terms of the mole ratio of TiO_2 to ZrO_2 in the nanocomposite structure, pH,

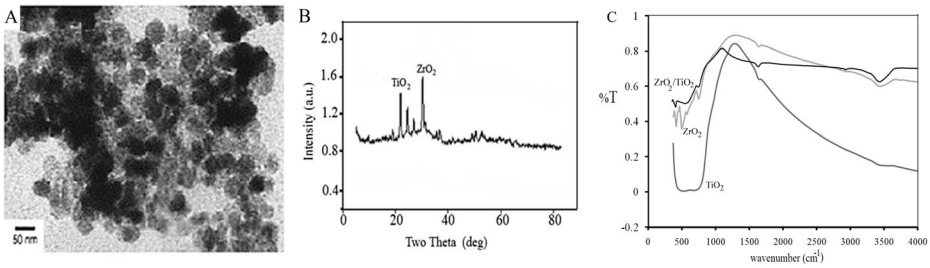

Fig. 1 **a** TEM image of ZrO_2/TiO_2 (1/1) calcined at 500 °C, **b** XRD pattern of the ZrO_2/TiO_2 (1/1) nanocomposite calcined at 500 °C, and **c** the FTIR spectra of TiO_2 nanoparticles, ZrO_2 nanoparticles, and ZrO_2/TiO_2 (1/1) mixed oxide

CHIT concentration, the mass of nanocomposite to MWNTs, the deposition time of the MWNTs-TiO_2/ZrO_2–CHIT on the surface of PGE, the electrostatic adsorption time of the ds-DNA, and DNA concentration on the Taxol response. To obtain the best conditions for the modified electrode, we optimized the ratio of TiO_2/ZrO_2 in nanocomposite structure. The best electrocatalytic effect for the determination of Taxol is obtained in ZrO_2–TiO_2 (1/1) nanocomposite. In fact, the grain size of the TiO_2-doped ZrO_2 is smaller than the undoped ZrO_2. Therefore, the effective area of the grain boundary per unit of the TiO_2-doped ZrO_2 is larger than that of the undoped ZrO_2 [27].

The influence of pH values on the electrochemical behavior of Taxol on the surface of the ds-DNA-MWNTs-TiO_2/ZrO_2–CHIT was studied between pH 4.0 and 10.0 by differential voltammograms. As shown in Fig. 2, the oxidation peak currents increased with the pH value from 3.0 to 7.0 and decreased at higher pH values indicating that ds-DNA-MWNTs-TiO_2/ZrO_2–CHIT exhibited excellent electrocatalytic performance toward Taxol oxidation at pH 7.0. Considering the best voltammetric responses of the ds-DNA-MWNTs-TiO_2/ZrO_2–CHIT-PGE and the physiological conditions, pH 7.0 was chosen as the most suitable pH value for investigating Taxol oxidation. With the increase in pH of the solution, peak potential shifted to less positive values obeying the following equation:

$$E_p(\mathrm{V}) = 1.6392 - 0.0612\,\mathrm{pH} \left(R^2 = 0.9865\right) \quad (1)$$

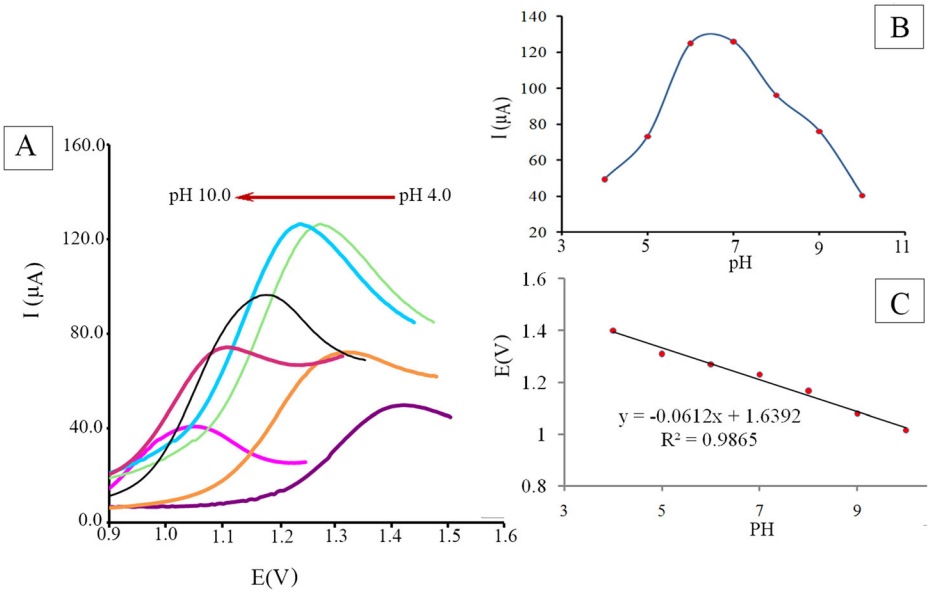

Fig. 2 **a** Effect of pH on the peak current and on the peak potentials of 700.0 nmol L^{-1} in phosphate buffer (0.1 mol L^{-1}) at ds-DNA-MWNTs-TiO_2/ZrO_2–CHIT modified pencil graphite electrode. Conditions: pulse amplitude 50 mV, pulse width 50 ms, and scan rate 100 mV s^{-1}. **b** Dependence of peak current on pH derived from the differential voltammograms data. **c** Dependence of peak potentials on pH derived from the differential voltammograms data

The slope of this equation suggests that the number of transferred electrons is equal to that of the hydrogen ions taking part in the electrode reaction:

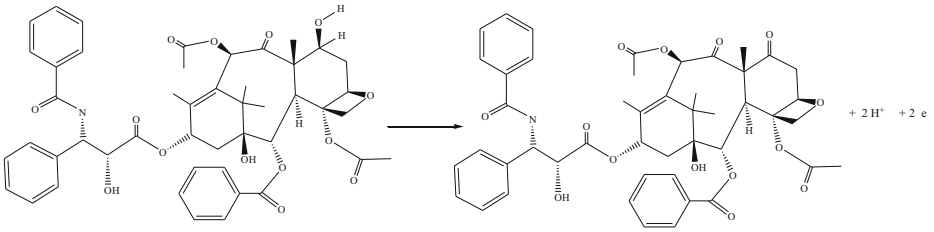

CHIT plays an important role in electrochemical sensing platform. So, the selection of CHIT concentration was investigated via differential concentrations, such as 0.5, 1, 2.0, and 2.5 %, respectively. DPVs currents of Taxol oxidation at each of the above electrodes were recorded. The optimal CHIT concentration was selected as 2 %.

The effect of the mass of TiO_2/ZrO_2 to MWNTs such as 1:1, 1:2, 1:3, 1:4, and 1:5 was examined. A small quantity of this nanocomposite brought a low immobilization amount of ds-DNA, while overflowing mass of TiO_2/ZrO_2 could contaminate the conductivity of the composite film. Thus, 1:2 was chosen.

The effect of the deposition time of the MWNTs-TiO_2/ZrO_2–CHIT on the surface of PGE for the electrochemical behavior of the Taxol was also studied. This investigation was performed by different deposition times (5, 10, 20, 30, and 40 min) in a 2 % chitosan solution containing MWNTs (1.0 mg mL^{-1}) and TiO_2/ZrO_2 nanocomposite (0.5 mg mL^{-1}). According to the obtained results, the peak current of Taxol is amplified at the first and then reaches a steady amount after 30 min. Thus, deposition time of 30 min was selected as the optimum time for the MWNTs-TiO_2/ZrO_2–CHIT deposition.

The electrostatic adsorption time of the ds-DNA had an obvious effect on DNA immobilization amount at ds-DNA-MWNTs-TiO_2/ZrO_2–CHIT pencil graphite electrode. When the electrode was soaked for 30 min or more, the peak current of Taxol on the modified PGE was stable, so 30 min was selected.

Low ds-DNA concentrations display no electrochemical signals at the PGE. This is mainly due to the mergence of anodic peak of oxidation bases and the background discharge. Therefore, 10 μg mL^{-1} of ds-DNA has been used for the construction of ds-DNA biosensor (Fig. 2).

Electrochemical Characterization of ds-DNA-MWNTs-TiO_2/ZrO_2–CHIT-PGE

MWNTs are not soluble in water and acid solution due to the aggregation caused by hydrophobic interaction and van der Waals attractive force between the nanotubes. However, carbon nanotubes investigate the role of the individual component, and the possible synergistic effects between MWNTs-TiO_2/ZrO_2 – CHIT, the CV responses of $[Fe(CN)_6]^{3-/4-}$ at the bare PGE, and different modified electrodes were studied as shown in Fig. 3a. It can be seen that a pair of obvious redox peak with I_{pa} of 97.3×10^{-6} A at +0.31 V and I_{pc} of 92.9×10^{-6} A at + 0.18 V appears at bare PGE. The peak currents of MWNTS–CHIT-PGE, I_{pa} of 126.0×10^{-6} A at 0.31 V, and I_{pc} of 118.0×10^{-6} A at +0.19 V increase because of larger specific surface area and good conductivity of MWNTs. However, the largest redox peaks (401.0×10^{-6} A at 0.28 V

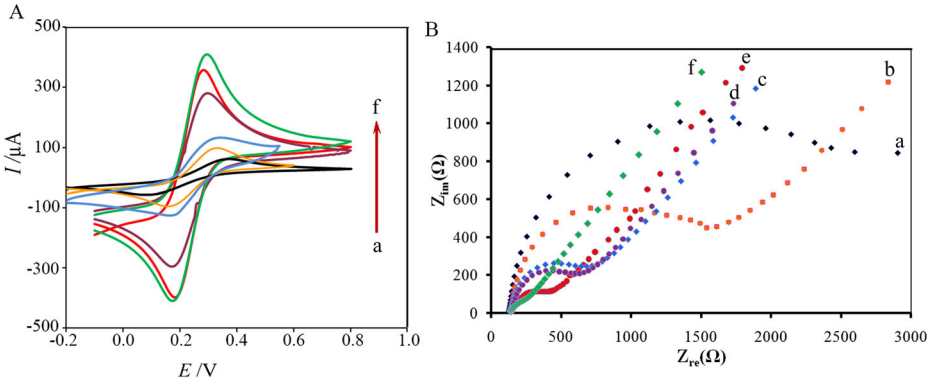

Fig. 3 **a** CVs and **b** impedance spectra of ds-DNA-MWNTs-TiO_2/ZrO_2–CHIT-PGE (*a*), unmodified PGE (*b*), MWNTs–CHIT-PGE (*c*), MWNTs-ZrO_2–CHIT-PGE (*d*), MWNTs-TiO_2–CHIT-PGE (*e*), and MWNTs-TiO_2/ZrO_2–CHIT-PGE in 5.0 mmol L^{-1} $[Fe(CN)_6]^{3-/4-}$ containing 0.1 mol L^{-1} KNO_3 (*f*). CV measurement at scan rate of 100 mV s^{-1} between −0.20 and +0.80 V and EIS. Conditions: polarization potential 0.15 V, frequency 5.0×10^{-3} to 10^5 Hz, and amplitude 10 mV

and I_{pc} of 402.7×10^{-6} A at +0.18 V) indicate that the synchronous introduction of MWNTs, TiO_2/ZrO_2, and CHIT would amplify the peak current of $[Fe(CN)_6]^{3-/4-}$ compared to bare PG electrode, MWNTs–TiO_2–CHIT-PGE, MWNTs–ZrO_2–CHIT-PGE, and MWNTs–CHIT-PGE. This could be ascribed to the effective integration of individual advantages of MWNTs and TiO_2/ZrO_2 nanocomposite and CHIT (such as large surface area, good catalytic activity, and excellent electrotronic conductivity), which revealed a synergistic effect in electrochemical response of $[Fe(CN)_6]^{3-/4-}$. In addition, the redox peak currents at MWNTs-TiO_2/ZrO_2–CHIT significantly changed as compared to redox peaks currents of $[Fe(CN)_6]^{3-/4-}$ at ds-DNA-MWNTs-TiO_2/ZrO_2–CHIT-PGE due to the repulsion between the negative charge of the phosphate groups of DNA and $[Fe(CN)_6]^{3-/4-}$.

In order to evaluate the electronic properties of the modified film, the electrochemical impedance spectroscopy (EIS) patterns of different electrodes in 0.1 mol L^{-1} KNO_3 containing $[Fe\ (CN)_6]^{3-/4-}$ as an electrochemical probe were recorded, as shown in Fig. 3b. The linear segment of the Nyquist plots at lower frequencies shows a controlled diffusion process, while the semicircular part at higher frequencies corresponds to the electron transfer limited process, and the diameter of the semicircle represents the electron transfer resistance. The Nyquist plot of bare PGE contains a clear semicircle and a linear feature. The decrease in the resistance value for the MWNTs–CHIT-PGE is attributed to the excellent conductive property of MWNTs. However, for the ds-DNA-MWNTs-TiO_2/ZrO_2–CHIT-PGE, there is a large well-defined arc in the high frequency section, indicating a huge interface electron transfer resistance. The result indicates that it is difficult for the negative probe to pass through the DNA film and access the electrode surface for exchanging electrons because of the existence of some electrostatic repulsion between DNA and $[Fe(CN)_6]^{3-/4-}$. This observation also confirms that DNA has been immobilized onto the electrode surface [28]. In the case of the MWNTs-TiO_2/ZrO_2–CHIT-PGE, the shape of the Nyquist plot is the same as that of the MWNTs-TiO_2–CHIT-PGE and MWNTs-ZrO_2–CHIT-PGE, but with a smaller semicircle diameter. These data indicate that the electron transfer resistance at the MWNTs-TiO_2/ZrO_2–CHIT-PGE surface is smaller than that in the other two electrodes, meaning that TiO_2/ZrO_2

nanocomposite shows unique properties compared to TiO_2 and ZrO_2 and that can promote the electron transfer and accelerate the ferricyanide diffusion toward the electrode surface (Fig. 3).

Figure 4a shows TEM images of ds-DNA-MWNTs-TiO_2/ZrO_2–CHIT hybrids on the surface of PGE. This picture shows that TiO_2/ZrO_2 is well distributed on the surface of MWNTs and also shows that MWNTs and TiO_2/ZrO_2 are distributed on the surface of PGE. MWNTs and TiO_2/ZrO_2 nanohybrid formed a porous structure which offered a good accessible surface area. It can also be noticed that the TiO_2/ZrO_2 nanocomposite onto the carbon nanotubes are spherical with average particle size of 30 nm.

Different tests were performed to examine the oxidation of Taxol under various electrode conditions. Figure 4b shows the oxidation differential pulse signals of 3000 nmol L^{-1}Taxol obtained at the different modified pencil graphite electrodes. The relationship between the type of nanoparticles and the oxidation peaks current of Taxol is seen in Fig. 4b. When CHIT was used as the dispersion of MWNTs and TiO_2/ZrO_2 as nanocomposite, the oxidation peak of Taxol increased. On the other hand, the oxidation peaks current of Taxol on the surface of ds-DNA-MWNTs-TiO_2/ZrO_2–CHIT-PGE increased by about 1.6 and 2.0 times vs. ds-DNA-MWNTs-TiO_2–CHIT-PGE and ds-DNA-MWNTs-ZrO_2–CHIT-PGE. It was found that the electrode modification with DNA and the nanostructure that dispersed in CHIT led to the enhanced sensitivity of Taxol voltammetric detection. This is due to the fact that surface immobilization of DNA plays an important role in the performance of DNA biosensors. The amount of the immobilized DNA probe will directly influence the accuracy, sensitivity, selectivity, and life of a DNA biosensor [25]. The MWNTs and TiO_2/ZrO_2 nanocomposite with their high surface-to-volume ratio and excellent biological compatibility can enlarge the sensing surface area that greatly increases the amount of immobilized DNA. The MWCNTs and TiO_2/ZrO_2 nanocomposite not only display unique electron transfer properties that induce

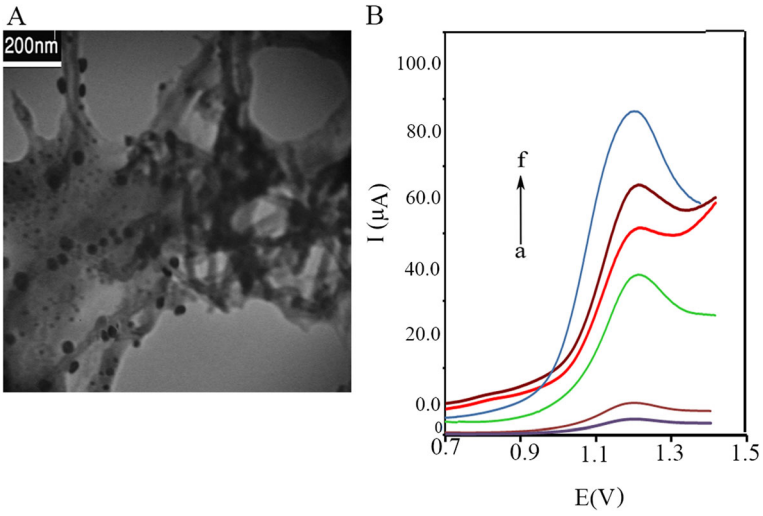

Fig. 4 **a** TEM images of ds-DNA-MWNTs-TiO_2/ZrO_2–CHIT modified pencil electrode. **b** The oxidation differential pulse signals of 3000 nmol L^{-1} Taxol obtained at the different electrodes: unmodified PGE (*a*), MWNTs–CHIT-PGE (*b*), ds-DNA-MWNTs–CHIT-PGE (*c*), ds-DNA-MWNTs-ZrO_2–CHIT-PGE (*d*), ds-DNA-MWNTs-TiO_2–CHIT-PGE (*e*), and ds-DNA-MWNTs-TiO_2/ZrO_2–CHIT-PGE (*f*). Conditions: pulse amplitude 50 mV, pulse width 50 ms, and scan rate 100 mV s^{-1}; phosphate buffer (0.1 mol L^{-1} at pH 7.0 containing 0.02 mol L^{-1} NaCl)

the conductivity of CHIT and improve electron characteristics but also increase the amount of CHIT (as a good matrix for DNA immobilization) on the surface of the electrode. In fact, the positively charged CHIT covers the surfaces of MWNTs and TiO_2/ZrO_2 nanocomposite by electrostatic interactions. Therefore, it is expected that the obvious increase in the detecting signal of Taxol oxidation is due to the enhanced immobilization of DNA in the case of ds-DNA-MWNTs-TiO_2/ZrO_2–CHIT-PGE. These results indicate a preconcentration of Taxol on the surface of ds-DNA-MWNTs-TiO_2/ZrO_2–CHIT-PGE due to its binding to ds-DNA. The plot of I_{pa} versus υ (scan rate) shows linear dependence of I_{pa} on υ. This behavior is consistent with adsorption of Taxol on the modified electrode (Figs. 4 and 5).

Interaction of ds-DNA with Taxol

Taxol was electrochemicaly oxidized at +1.18 V in the phosphate buffer pH 7.4 at the bare pencil graphite electrode by differential pulse voltammetry, while pure ds-DNA displayed no electrochemical signals at PGE at low concentrations. Figure 6a shows the behaviors of 2000 nmol L^{-1} Taxol in the absence and presence of ds-DNA and ss-DNA at pH 7.4. The anodic peak potential (E_{pa}) in the presence of ds-DNA is located at +1.21 V with a decrease in the peak current, while no obvious changes have been shown in the presence of ss-DNA. Based on these observations, it seems that the decrease in the peak current of Taxol upon ds-DNA addition is due to the binding of Taxol with bulky and slowly diffusing ds-DNA.

The technique of differential pulse voltammetry (DPV) was employed in order to further confirm the interaction of ds-DNA with Taxol. The optimized experimental conditions for DPV were as follows: pulse amplitude 50 mV, pulse width 50 ms, and scan rate 100 mV s^{-1}. Figure 6b shows the DPVs of 2000 nmol L^{-1} Taxol in 0.1 M phosphate buffer pH 7.4 solution in the presence of ds-DNA with different concentrations. As it could be seen, by adding ds-DNA into Taxol solution, the peak currents of Taxol gradually decreased with a positive shift

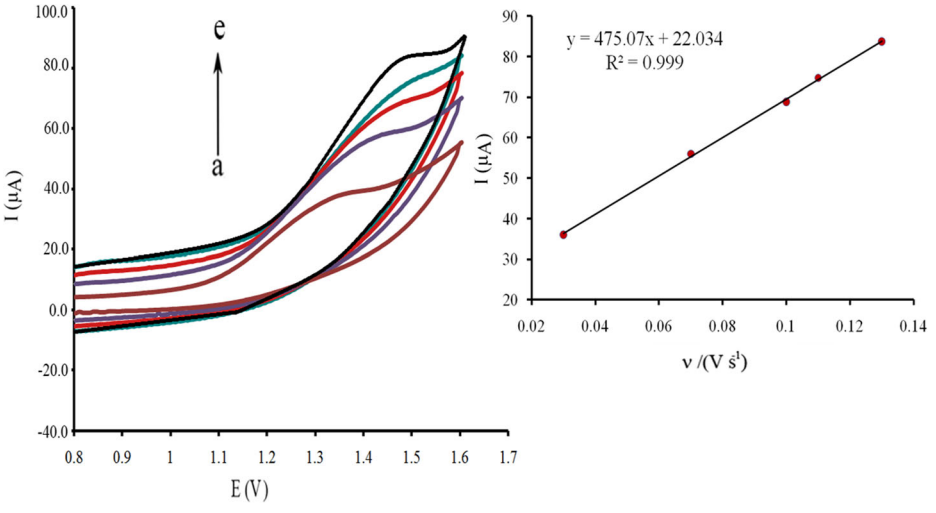

Fig. 5 Cyclic voltammograms of 500 nmol L^{-1} Taxol (pH 7.0) on the surface of ds-DNA-MWNTs-TiO_2/ZrO_2–CHIT modified pencil electrode at various scan rates: 30 (*a*), 70 (*b*), 100 (*c*), 110 (*d*), and 130 mV s^{-1} (*e*)

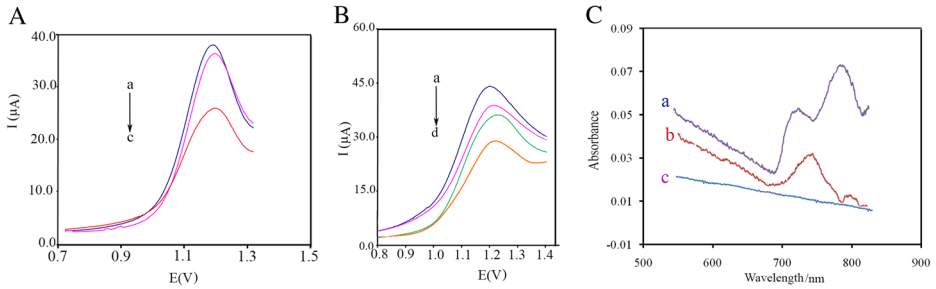

Fig. 6 **a** DPVs of Taxol at the unmodified PGE in phosphate buffer solution (0.1 mol L^{-1} at pH 7.4); 2000 nmol L^{-1} Taxol (*a*), 2000 nmol L^{-1} Taxol and 10.0 μg mL^{-1} ss-DNA (*b*), and 2000 nmol L^{-1} Taxol and 10.0 μg mL^{-1} ds-DNA (*c*). **b** DPVs of 2000 nmol L^{-1} Taxol at the unmodified PGE in phosphate buffer solution (0.1 mol L^{-1} at pH 7.4 containing 0.02 mol L^{-1} NaCl) with different concentrations of the ds-DNA: 0.0 (*a*), 5.0 (*b*), 10.0 (*c*), and 20.0 μg mL^{-1} (*d*). Conditions: pulse amplitude 50 mV, pulse width 50 ms, and scan rate 100 mV s^{-1}; phosphate buffer (0.1 mol L^{-1} at pH 7.0 containing 0.02 mol L^{-1} NaCl). **c** UV spectra of 2000 nmol mL^{-1} Taxol in Tris buffer solution (pH 7.4) (*a*), 10.0 μg mL^{-1} ds-DNA interacting with 2000 nmol mL^{-1} Taxol after 10 min in Tris buffer solution (pH 7.4) (*b*), and 10.0 μg mL^{-1} ds-DNA in Tris buffer solution (pH 7.4) (*c*)

(about 30 mV), which strongly confirmed groove binding interaction of Taxol with ds-DNA [28].

UV-Vis absorption is one of the spectroscopic techniques generally employed to investigate drug-DNA interactions. The absorption spectrum of Taxol exhibited bands at 227, 718, and 780 nm (Fig. 6c), and the peak position of the ds-DNA appeared at 260 nm [17]. Bands were selected at 718 and 780 nm to investigate the interaction between DNA and Taxol. The absorbance of Taxol decreased at 718 and 780 nm (with red shift) by adding ds-DNA. Therefore, the groove binding of molecules to ds-DNA helix has been proved because of a red shift ($\Delta\lambda \leq 8$ nm)[29] (Fig. 6).

Repeatability and Stability

The repeatability and stability of the ds-DNA-TiO_2/ZrO_2-MWNTs–CHIT-PGE were also evaluated. The negligible current change in response to Taxol was observed, after 90 times of recycling. The relative standard deviation (R.S.D.) for current determination of Taxol was less than 8 % for six modified electrodes. The stability of the modified PGE was also estimated every 3 days, and it remained 90 % of its initial current response for Taxol over a month. The results indicate that ds-DNA-TiO_2/ZrO_2-MWNTs–CHIT-PGE is a stable and efficient electrochemical sensor for the detection of Taxol.

Calibration Curve and Detection Limit

Differential pulse voltammetry was used to determine Taxol concentration in aqueous solutions with optimum conditions. Results showed a linear segment for Taxol concentration; namely, for 0.70 to 1874.0 nmol L^{-1} of Taxol, the regression equation was $\Delta I_p(\mu A)=(0.1527 \pm 0.001)\ C_{Taxol}+(8.634\pm0.50)$ (R^2=09938, n=5) (Fig. 7), where C_{Taxol} concentration is in nanomoles per liter. The detection limit (defined as $3s_b/m$, where s_b is the standard deviation of

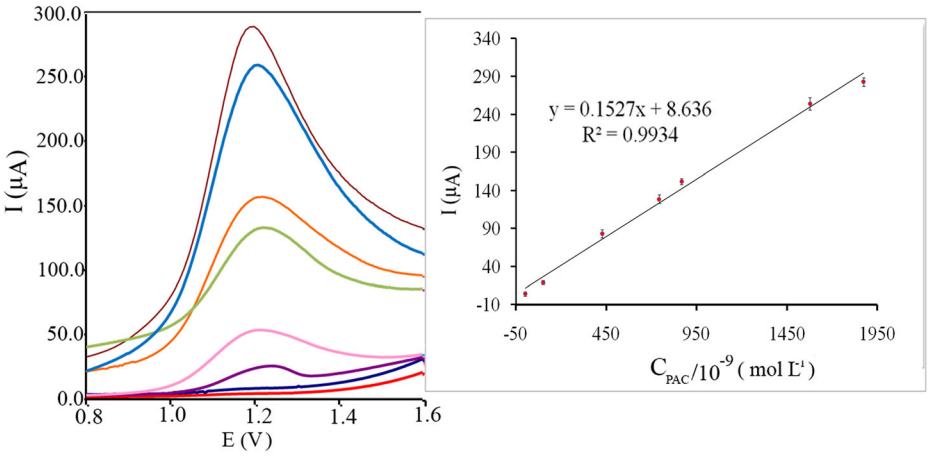

Fig. 7 Calibration curve for the determination of Taxol based on preconcentrated oxidation signal of Taxol at MWNTs-TiO_2/ZrO_2–CHIT-PGE. DPVs of 0.0, 0.7, 100.0, 427.0, 742.0, 867.0, 1578.0, and 1874.0 nmol L^{-1} Taxol (the *error bars* are standard deviations for n=5) (*inset*). Conditions: pulse amplitude 50 mV, pulse width 50 ms, and scan rate 100 mV s^{-1}; phosphate buffer (0.1 mol L^{-1} at pH 7.0 containing 0.02 mol L^{-1} NaCl)

the blank signal (n=5) and m is the slope of the calibration curve) was found to be 0.010 nmol L^{-1} (Fig. 7).

Interference Study

The effect of various potential interferences on the signal of oxidation of 50 nmol L^{-1} Taxol was studied under optimum conditions at pH 7.0. The tolerance limit was defined as the

Table 1 Determination of Taxol in real samples

Real sample	Added (nmol L^{-1})	Proposed method (nmol L^{-1})	Recovery (%)	Official method (nmol L^{-1})
Urine 1	30.0	30.8 (±3.00)	–	30.7 (±1.59)
Urine 2	200.00	209.1 (±5.50)	104.5	–
	1000.0	1188.4 (±14.7)	99.0	–
Serum 1	10.0	9.7 (±0.60)	97.0	9.9 (±0.33)
	100.0	103.2 (±3.2)	93.9	–
	50.0	156.4 (±1.80)	97.8	–
Serum 2	500.0	505.5 (±11.3)	101.1	–
	30.0	510.7 (±10.1)	96.4	–
	70.0	573.3 (±7.7)	95.6	–
Taxol drug injection[a]	–	481.4 (±10.27)	–	490.4 (±3.59)
	40.0	518.7 (±8.42)	97.8	–
	200.0	701.2 (±40.37)	96.0	–

Number in the parenthesis shows the standard deviation of n=5

[a] Taxol injection solution sample 6 mg mL^{-1}, Bristol-Myers Squibb

maximum concentration of the interfering substance that caused an error less than ±5 % for the determination of Taxol. The results showed that 1000-fold of Na^+, Br^-, F^-, Mg^{2+}, Ca^{2+}, K^+, NO_3^-, and NO_2^-, 600-fold of SO_4^{2-} and glucose, 500-fold of fructose, sucrose, lactose, urea, and aspartic acid, and 200-fold of citrate did not affect the signal of Taxol. The result shows that only ascorbic acid could be an interference for the determination of Taxol using this modified electrode. This interference can be minimized by using ascorbic oxidase enzyme, which exhibits high selectivity to oxidation of ascorbic acid if necessary.

Analytical Applications

The practical application of ds-DNA-TiO_2/ZrO_2-MWNTs–CHIT-PGE was tested by measuring the concentrations of Taxol in ampules and human biological samples. The Taxol ampules were analyzed directly after being suitably diluted with the buffer solution (pH 7.0). The average determination results of Taxol in the injection samples were quite corresponding to the value given by injection specifications. This produce was repeated five times, and the relative standard deviation obtained was 5.60 %. Different standard concentrations of Taxol were added to the diluted Taxol injection, and the recovery was between 93.9 and 104.5 % for five measurements.

In order to evaluate the analytical applicability of the proposed method, it was also applied to the determination of Taxol in human blood serum and urine samples. The results , as presented in Table 1, show very good recoveries for determination of Taxol with high reproducibility. In addition, comparisons of the proposed method with official methods [30] also confirmed the accuracy of the results obtained by our proposed method, showing no significant differences from those of the standard method.

Conclusion

The present study demonstrates the construction of the TiO_2/ZrO_2 nanocomposite. After characterization of TiO_2/ZrO_2 nanocomposite, a sensitive DNA-biosensor was developed for the determination of Taxol in biological and injection samples based on the combination of TiO_2/ZrO_2 nanocomposites with MWNTs in the matrix of biopolymer CHIT. Using the ds-DNA-TiO_2/ZrO_2-MWNTs–CHIT-PGE, we were able to detect the interaction of Taxol with ds-DNA, which allowed us to apply a DNA-modified electrode for ultra-trace determination of Taxol. The resulting ds-DNA-TiO_2/ZrO_2-MWNTs–CHIT-PG electrode shows good characteristics such as a large determination range, good sensitivity, fast response time, high stability, and excellent selectivity.

References

1. Rao, C. N. R., Satishkumar, B. C., Govindaraj, A., & Nath, M. (2001). Nanotubes. *ChemPhysChem, 2*, 78–105.
2. Baughman, R. H., Zakhidov, A., & de Heer, W. A. (2002). Carbon nanotubes–the route toward applications. *Science, 297*, 787–792.

3. Ensafi, A. A., Khoddami, E., Rezaei, B., & Karimi-Maleh, H. (2010). *p*-Aminophenol–multiwall carbon nanotubes–TiO_2 electrode as a sensor for simultaneous determination of penicillamine and uric acid. *Colloids and Surfaces B, 81*, 42–49.
4. Adekunle, A. S., Agboola, B. O., Pillay, J., & Ozoemena, K. I. (2010). Electrocatalytic detection of dopamine at single-walled carbon nanotubes–iron (III) oxide nanoparticles platform. *Sensors and Actuators B, 148*, 93–102.
5. Dong, Y., & Zheng, J. (2014). A nonenzymatic l-cysteine sensor based on SnO_2-MWCNTs nanocomposites. *Journal of Molecular Liquids, 196*, 280–284.
6. Liu, Z., Zhai, H., Chen, Z., Zhou, Q., Liang, Z., & Su, Z. (2014). Simultaneous determination of orange G and orange II in industrial wastewater by a novel Fe_2O_3/MWCNTs-COOH/OP modified carbon paste electrode. *Electrochimica Acta, 136*, 370–376.
7. Zhang, L., Xu, L., He, J., & Zhang, J. (2014). Preparation of Ti/SnO2-Sb electrodes modified by carbon nanotube for anodic oxidation of dye wastewater and combination with nanofiltration. *Electrochimica Acta, 117*, 192–201.
8. Mehdinia, A., Ziaei, E., & Jabbari, A. (2014). Multi-walled carbon nanotube/SnO_2 nanocomposite: a novel anode material for microbial fuel cells. *Electrochimica Acta, 130*, 512–518.
9. Huo, D., Li, Q., Zhang, Y., Hou, C., & Lei, Y. (2014). A highly efficient organophosphorus pesticides sensor based on CuO nanowires–SWCNTs hybrid nanocomposite. *Sensors and Actuators B, 199*, 410–417.
10. Liu, Y., Tang, J., Chen, X., & Xin, J. H. (2005). Decoration nanotubes with chitosan. *Carbon, 43*, 3178–3180.
11. Pauliukaite, R., Ghica, M. E., Fatibello-Filho, O., & Brett, C. M. A. (2009). Comparative study of different cross-linking agents for the immobilization of functionalized carbon nanotubes within a chitosan film supported on a graphite− epoxy composite electrode. *Analytical Chemistry, 81*, 5364–5372.
12. Li, J., Liu, Q., Liu, Y., Liu, S., & Yao, S. (2005). DNA biosensor based on chitosan film doped with carbon nanotubes. *Analytical Biochemistry, 346*, 107–114.
13. Ensafi, A. A., Amini, M., & Rezaei, B. (2014). Impedimetric DNA-biosensor for the study of anti-cancer action of mitomycin C: comparison between acid and electroreductive activation. *Biosensors & Bioelectronics, 59*, 282–288.
14. Saville, M. W., Lietzau, J., Pluda, J. M., Wilson, W. H., Humphrey, R. W., Feigel, E., Steinberg, S. M., & Broder, S. (1995). Treatment of HIV-associated Kaposi's sarcoma with paclitaxel. *The Lancet, 346*, 26–28.
15. Mehdinia, A., Kazemi, S. H., Bathaie, S. Z., Alizadeh, A., Shamsipur, M., & Mousavi, M. F. (2008). Electrochemical studies of DNA immobilization onto the azide-terminated monolayers and its interaction with taxol. *Analytical Biochemistry, 375*, 331–338.
16. Holgado, T. M., Quintana, M. C., & Pinilla, J. M. (2003). Electrochemical study of taxol (paclitaxel) by cathodic stripping voltammetry: determination in human urine. *Microchemical Journal, 74*, 99–104.
17. Cheng, W. X., Peng, D. Y., Lu, C. H., & Fang, C. W. (2008). Direct electrochemical behavior of the Cysteamine/DNA/SWNTs-film-modified Au electrode and its interaction with taxol. *Russian Journal of Electrochemistry, 44*, 1052–1057.
18. Gowda, J. I., & Nandibewoor, S. T. (2014). Electrochemical characterization and determination of paclitaxel drug using graphite pencil electrode. *Electrochimica Acta, 116*, 326–333.
19. Zhang, Y., Cheng, W., Li, S., & Li, N. (2006). Direct electron transfer of hemoglobin on DDAB/SWNTs film modified Au electrode and its interaction with Taxol. *Colloids and Surfaces, A, 286*, 33–38.
20. Yu, Y., & Li, Q. (2001). Studies on the interaction of paclitaxel with tubulin by an electrochemical method. *Analytica Chimica Acta, 436*, 147–152.
21. Gowda, J. I., & Nandibewoor, S. T. (2014). Electrochemical behavior of paclitaxel and its determination at glassy carbon electrode. *Asian Journal of Pharmaceutical Sciences, 9*, 42–49.
22. Ghiaci, M., Aghaei, H., & Abbaspur, A. (2008). Size-controlled synthesis of ZrO"$_2$-TiO"$_2$ nanoparticles prepared via reverse micelle method. *Materials Research Bulletin, 43*, 1255–1262.
23. Wang, L., Xiong, H., Zhang, X., & Wang, S. (2009). Electrochemical behaviors of nicotine and its interaction with DNA. *Electrochemistry Communications, 11*, 2129–2132.
24. Ghiaci, M., Abbaspur, A., & Kalbasi, R. J. (2005). Vapor-phase Beckmann rearrangement of cyclohexanone oxime over H_3PO_4/ZrO$_2$–TiO$_2$. *Applied Catalysis A, 287*, 83–88.
25. Ensafi, A. A., Amini, M., & Rezaei, B. (2013). Biosensor based on ds-DNA decorated chitosan modified multiwall carbon nanotubes for voltammetric biodetection of herbicide amitrole. *Colloids and Surfaces, B, 109*, 45–51.
26. Kim, J. Y., Kim, C. S., Chang, H. K., & Kim, T. O. (2011). Synthesis and characterization of N-doped TiO"$_2$/ZrO"$_2$ visible light photocatalysts. *Advanced Powder Technology, 22*, 443–448.
27. Tekeli, S., Akçimen, A., Gürdal, O., & Gürü, M. (2007). Microstructural and electrical conductivity properties of cubic zirconia doped with various amount of titania. *Journal of Achievements in Materials and Manufacturing Engineering, 25*, 39–42.

28. Sirajuddin, M., Ali, S., & Badshah, A. (2013). Drug-DNA interactions and their study by UV-Visible, fluorescence spectroscopies and cyclic voltametry. *Journal of Photochemistry and Photobiology B: Biology, 124*, 1–19.
29. Ensafi, A. A., Heydari-Bafrooei, E., & Amini, M. (2012). DNA-functionalized biosensor for riboflavin based electrochemical interaction on pretreated pencil graphite electrode. *Biosensors & Bioelectronics, 31*, 376–381.
30. Sparreboom, A., de Bruijn, P., Nooter, K., Loos, W. J., Stoter, G., & Verweij, J. (1998). Determination of paclitaxel in human plasma using single solvent extraction prior to isocratic reversed-phase high-performance liquid chromatography with ultraviolet detection. *Journal of Chromatography B: Biomedical Sciences and Applications, 705*, 159–164.